Posture-invariant hybrid scaling weight measurement algorithm for live eels

Qing Liu[1], Yuxing Han[2], Guoqi Yan[1,3*], Jiasi Mo[1], Zishang Yang[2]

(1. *College of Engineering, South China Agricultural University, Guangzhou 510642, China*;
2. *College of Electronic Engineering, South China Agricultural University, Guangzhou 510642, China*;
3. *Maoming Branch, Guangdong Laboratory for Lingnan Modern Agriculture, Maoming 525000, Guangdong, China*)

Abstract: To obtain higher economic benefits, large eel breeding companies classify live eels by weight. Due to their strong mobility and smooth body surface, living eels are not suitable for traditional mechanical weight measurement. In this study, a live eel sorting machine based on machine vision was developed, and a novel method was developed for obtaining live eel weight measurements through images. First, a backlit workbench was designed to capture static images of eels, and then the projection area and skeleton length of the images were obtained by image preprocessing. For the eel's body shape, which is generally cylindrical and gradually transitions to a flat tail, the tail posture changes affect the shape of the images; thus, a weight measurement model combining the projected area and the skeleton length was proposed. The optimal scale division coefficient of the weight model was found to be 0.745 by experimentation. Then, select eels of different weight ranges were used for model error verification and to obtain the correction function of the error. The weight gradient was used to confirm the corrected eel weight model. Finally, the system calculation results were compared with the actual measurement results. The root mean square error (RMSE) was 12.94 g, and the mean absolute percentage error (MAPE) was 2.12%. The results show that the proposed method provided a convenient, fast, and low-cost non-contact weight measurement method for live eels, reduced the damage rate of live eels, and can meet the technical requirements of actual production.

Keywords: scale factor, weight measurement, non-contact, live eels
DOI: 10.25165/j.ijabe.20231602.7132

Citation: Liu Q, Han Y X, Yan G Q, Mo J S, Yang Z S. Posture-invariant hybrid scaling weight measurement algorithm for live eels. Int J Agric & Biol Eng, 2023; 16(2): 207–215.

1 Introduction

In recent years, with the continuous improvement of people's living standards, consumers' requirements for food quality have become higher and higher. Eel is becoming more and more popular as a food with rich value in nutrition. Optimization and evaluation of eel grade are one of the ways to improve its economic efficiency. The traditional classification of eels is mainly manual and classified into different grades according to their weight[1]. This method relies mainly on the experience of workers, in which the weight of eels is judged by the eyes of workers, and this grading method is labor-intensive, with low grading efficiency and accuracy, and for large breeding enterprises, the long manual sorting time and the rate of dead fish will increase significantly, reducing the economic efficiency of the product, which is not conducive to the rapid development of the eel industry. Meanwhile, the traditional mechanical motion weighing method may damage live eels due to their strong mobility and smooth surface.

In recent years, with the rapid development of machine vision and image processing technologies, various vision-based inspection methods have been widely used[2-4]. Vision-based yield and weight estimation and classification have become a popular research direction in the last decade[5-9]. The non-contact, fast, and low-cost characteristics of computer vision technology make automatic image-based weight measurement possible[10,11], Zhang et al.[12] used machine vision to achieve weight detection of three common freshwater fish, they divided the fish into three parts: head, body, and tail, and then based on the proportion of the projected area of each part to the overall fish body and the weight proportion, the test showed that the weight of the fish was highly correlated with the projected area, and the error of this quality detection model was 3.89%. Li et al.[13] applied the computer vision technology in fish grading and sorting, used crucian carp as the research object, and found that the correlation between the power function of fish length and weight was high through image processing and calculation, and proposed a classification method to calculate weight using body length to achieve grading of crucian carp. Viazzi et al.[14] used 2D computer vision technology by extracting the length and width of the jade perch in the image establishing shape and group mass estimation for this fish. Ma et al.[15] used machine vision techniques to obtain images of narrow-bodied tongue sole individuals, measured the area of irregular images by digital image processing techniques, and used linear regression techniques to establish the correspondence between the image area and body weight, and the correlation coefficient between projected area and weight was 0.3807 as indicated by data analysis. Wang et al.[16] combined depth images and BP neural networks to establish a broiler body mass estimation model, and the acquired images were processed to extract the projection area, eccentricity, perimeter, target volume,

Received date: 2021-10-17 **Accepted date:** 2022-09-19
Biographies: Qing Liu, Master, research interest: application of machine vision in agriculture, Email: lq@stu.scau.edu.cn; **Yuxing Han**, PhD, Professor, research interest: electronic information communication, Email: yuxinghan@sz.tsinghua.edu.cn; **Jiasi Mo**, PhD, Lecturer, research interest: agricultural robot, Email: mo_jiasi@scau.edu.cn; **Zishang Yang**, PhD, research interest: machine vision, Email: yzs@stu.scau.edu.cn.
***Corresponding author: Guoqi Yan**, PhD, Associate Professor, research interest: aquaculture and primary processing equipment research. College of Electronic Engineering, South China Agricultural University, Guangzhou 510642, China. Tel: 13826492989, Email: ygq1978@scau.edu.cn.

length value, width value, back width, and other features of the broiler images to establish a broiler mass model to achieve broiler mass detection, and the experimental results showed that the average relative error of broiler mass detected by this method was 0.0010-0.0628 kg range, and the best fit reached 0.9943. De Wet et al.[17] studied the correlation between surface area and perimeter of broiler images and body mass using image processing techniques, and the results were obvious. The projected area in the broiler depth image refers to the area of the largest target in the image, and the summation of the number of pixels at the boundary points can be used as the perimeter. Schofiled et al.[18] built an automatic image acquisition and analysis system in an actual pig farm, using image processing techniques to obtain dorsal area and a prediction model between it and body mass, and successfully recorded the growth records of three breeds of pigs. Yang et al.[19,20] used the projected area of breeding pigs to predict their body mass by digital image analysis technique, and the relative error of the prediction result was less than 2.8% compared with manual measurement. Alikhanov et al.[21] proposed a method for egg weight classification and grading using machine vision technology, using regression analysis to establish the relationship between egg weight and egg geometric parameters perimeter, area, size axis, shape index, and shape factor. The experimental results showed that the most important parameter related to egg weight was egg area with a correlation coefficient of 0.989, defining an egg weight area The mathematical model of the relationship was determined with a coefficient of 0.978 and a total classification error of 2.5%. Wang et al.[22] explored the application of computer vision technology for mango weight detection, using a charge-coupled device camera to ingest mango images, and establishing the correlation between fruit weight and its projected image by obtaining the horizontal projected area (total number of pixels) of mangoes in their naturally placed state, and experimentally demonstrating that computer vision achieved 96% accuracy in grading the fruit weight detection of Gui Xiang mangoes and 92% accuracy in grading the fruit weight detection of purple flower mangoes. Kalantar et al.[23] developed a method for melon weight estimation based on unmanned aerial vehicle images, first, using RetinaNet to achieve melon target detection from unmanned aerial vehicle images, then based on contour and principal component analysis algorithms to achieve melon feature extraction, and finally, establishing a regression model for single melon weight estimation to achieve melon yield estimation.

The works mentioned above are summarized in Table 1. Although vision-based weight inspection methods are widely used, few have applied vision inspection to live eel weight estimation. In contrast, the use of machine vision technology for eel grading does not need to consider the influence of eel motion on grading accuracy, can achieve non-contacting, and is more adaptable compared to traditional conventional mechanical motion weighing methods. Therefore, this study proposed a novel method for measuring the weight of live eels by images.

Table 1 Overview of studies on machine vision in weight detection

Species	Parameters of interest	Deliverable	Reference
Fish	Projected area of fish head, fish body, and fish tail	Quality detection model of weight and projected area	[12]
	Body length	Correlation function of body length and weight	[13]
	Length and width of fish	Estimation models for length and width and weight	[14]
	Area of the image	Correspondence between image area and body weight	[15]
Chicken	Image projected area, eccentricity, perimeter, target volume, length value, width value, back width	Broiler quality model	[16]
	Image surface area, perimeter (the number of pixels in the boundary point)	Surface area and perimeter as a function of weight	[17]
Pig	Rear projection area	Estimated model between back projected area and mass	[18]
	Shadow area	Body mass prediction model	[19,20]
Egg	Perimeter, area, size axis, shape index, and shape factor	Mathematical model of the relationship between egg weight and area	[21]
Mango	Horizontal projection area(total pixels)	The relationship between fruit weight and its projected image	[22]
Melon	Contour, principal component	Single melon weight estimation regression model	[23]

Consistent with previous work, based on the developed live eel sorting machine, this study presented a method for obtaining the weight of live eels using images. The method did not require complex electromechanical weight detection devices, effectively reduced the damage rate of live eels, and met the practical needs of factory production. The development of the method includes 1) Designing a backlit eel image acquisition bench; 2) Obtaining the projection area and skeleton length of eel images through image preprocessing; 3) Indicating that the eel body is roughly cylindrical and gradually transitions to a flat tail, proposing a weight measurement method combining projection area and skeleton length, and establishing an eel weight detection model through eel segmentation experiments; 4) Selecting eels of the different weight ranges of eels for model error verification to obtain the corrected mathematical model of eel weight; 5) The system calculation results were compared with the actual measurement results to verify the corrected mathematical model of eel weight. This study provided a convenient, fast, and low-cost method for the non-contact weight measurement of live eels.

2 Materials and methods

This study was based on the live eel sorting machine developed by a school-enterprise cooperation project. The sorting machine aimed to separate eels by weight through a mechanical method instead of a manual method to meet the requirements of export. The sorting machine was manually loaded, and then the weight of the eel was estimated by machine vision, and then the eel was dropped into different grades of barrels by weight through the mechanical sorting door. The sorting machine can be divided into 5 levels according to the required weight, and its structure is shown in Figure 1.

2.1 Experimental design and data acquisition

Preliminary image acquisition experiments showed that the acquisition box of the eel's production factory was made of stainless steel. Under natural or artificial light sources, strong reflections will appear on the bottom of the acquisition box during

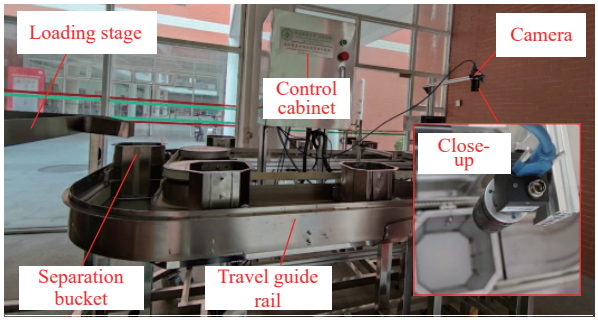

Figure 1 Structure of living eel sorting machine

the image acquisition process, and the surface of the living eel will also appear as a reflection, which affects the quality of the captured image. The image collected by the stainless-steel acquisition box of the factory is shown in Figure 2a.

a. Stainless steel b. Backlit

Figure 2 Comparison of two types of data acquisition box

At the same time, due to the long-term inspection needs of the eel production line in the factory, the changes in the external light source will cause interference problems in the collected images. Choosing more cumbersome image processing methods will slow down the calculation speed and affect the real-time performance of the entire inspection process. Therefore, a live eel image acquisition device based on back-lighting was designed. Backlight transmission was used to collect two-dimensional (2D) projection images of eels to solve the problems of the instability of external light sources and reflection interference. An image of the designed acquisition box is shown in Figure 2b.

The size of the backlit acquisition workbench was 600×800 mm², and the type of lights was YR-52T. The experimental data were collected by a USB industrial camera with 2 million pixels, a lens with a fixed focal length of 6 mm was used, the exposure was set to automatic, and the resolution of the collected image was 1280×960 pixels. The industrial camera was placed 800 mm above the workbench (Figure 3). To collect images as close to the real production environment as possible, live eels (*Anguilla japonica*) were randomly selected as experimental objects. Each live eel was randomly placed on the workbench, and images of different poses of the same live eel were collected multiple times. After the image acquisition was complete, an electronic scale was used to manually measure the weight of each eel.

To obtain the size relationship between the image and the real space, a certain size reference object (76×76 mm²) was placed beside the eels during the image acquisition process. By comparing the size of the reference object between the image and the real world, the size of the eels in the real world could be determined.

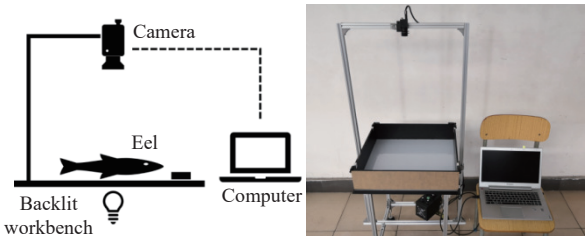

Figure 3 Data acquisition system.

2.2 Image data processing pipeline

2.2.1 Image preprocessing

To realize the image-based eel weight measurement, the eel's image was first segmented. The main methods of identifying fish in images are shape-based analysis and color-based analysis. Considering that the backlight method was used to collect the image, the eel area had significant characteristics in the image; therefore, the color-based analysis method was used in this study[24,25].

First, the color image of the eel was converted into a gray image, and then the adaptive threshold method was used for segmentation[26]. The grayscale image was converted into a binary image through the adaptive threshold. After image segmentation, some noise could still be found in the image, and, to eliminate this noise, a morphological operation was performed to obtain an accurate eel image pixel set. Figure 4a is the original image, and Figure 4b is the processed binarized image.

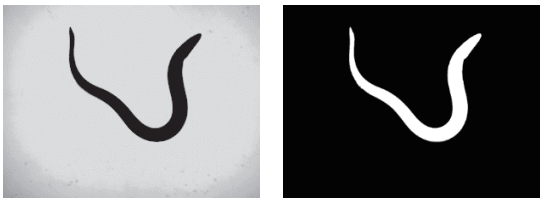

a. Original image b. Proccessed binarized image

Figure 4 Eel projection image and binarized image

2.2.2 Acquisition of projected area

For the obtained binary images of eels, the pixel area with a gray value of one represents the target area of the eel. Therefore, the pixel area of the eel in the image can be obtained by calculating the number of pixels with a gray value of one in the image. Figure 5a shows the eel area. To calculate the projected area of irregular objects, the calibration method is typically used[27]. First, the experimental object and a fixed-size reference object were placed on the background board. Then the image area of the experimental object and the reference object were calculated, and the reference object was used to calculate the relationship between a single pixel and the actual area. The actual area of the test object was obtained by the product of its own image area and this relationship. Figure 5b is the image area of the reference object. The calculation equation for the real-world area of the eel is

$$S_{\text{ref}} = k_s S'_{\text{ref}} (1) \tag{1}$$

where, S_{ref} represents the real-world area, mm²; S'_{ref} represents the image-world area, pixel²; k_s=S_{ref}/S'_{ref} represents the area scale factor between the real-world and the image-world, mm/pixel.

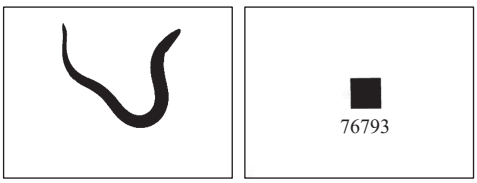

a. Test object b. Fixed size reference object

Figure 5 Area calculation of the eel projection image

2.2.3 Acquisition of skeleton length

For the eel image, because the shape is non-linear, it is difficult

to calculate its length directly from the image. Therefore, this study first extracted the eel skeleton and then used the measured length of the skeleton as the eel's body length. The specific method involved first calculating the contour map of the eel. For the binarized eel image, the number of neighborhood points of its contour pixels was less than eight; thus, the number of neighborhoods of the image was traversed at the same time to realize the calculation of the contour map as shown in Figure 6a. On this basis, the sequential iterative algorithm was used to obtain the morphological skeleton through the contour map of the eel image as shown in Figure 6b.

a. Contour map of the eel image b. Morphological skeleton from the contour map

Figure 6 Extraction of the eel skeleton

For the obtained eel skeleton, the Manhattan distance was calculated as the length. The calculation formula for the real-world size of the eel length is:

$$L = k_l L' = \sqrt{k_s} L' \tag{2}$$

where, L represents the real length of the eel, cm; L' represents the image world distance of the ell, pixel; $k_l = L_{ref}/L'_{ref}$ represents the length scale factor between the real world and the image world, cm/pixel.

2.3 Establishment of eel weight model

2.3.1 Eel weight analysis

The eel has a slender body, a flattened and tapered head, a nearly cylindrical body, and a high content of muscle and fat. When stimulated from the outside, the body of the fish shrinks most obviously close to the tail, the body gradually shrinks from both sides to the middle, the thickness of the fish body decreases, the content of muscle and fat becomes less apparent, and the tail becomes slightly flat. Figure 7 shows the different forms of the same eel, where Figure 7b is the state of the fish body when it contracts.

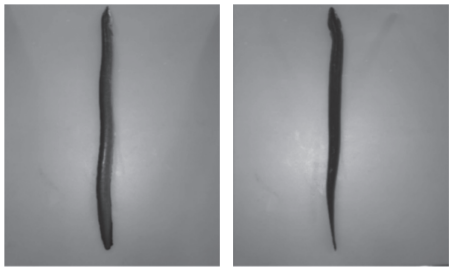

a. Eel body b. state of the eel body when it contracts

Figure 7 Physical image of live eels

At the same time, affected by the changes in the movement of the living eel, the posture of its tail causes the area of the projected image to change. Figure 8a shows the eel tail posture when perpendicular (vertical) to the camera, and Figure 8b shows the eel tail posture when parallel (flat) to the camera. The projected area of the tail of the middle eel is smaller than that of Figure 8b, and the projected area of the front of the eel is almost unchanged.

a. Tail posture when perpendicular (vertical) to the camera b. Tail posture when parallel (flat) to the camera

Figure 8 Comparison of the different postures of eel tails

In summary, the area of the projected image of the same eel will change significantly under different conditions. Therefore, it is unreliable to establish the relationship between the weight and the image through simple regression analysis. At the same time, inspired by the changes in eel morphology, an eel weight model based on a combination of the projected area and skeleton length was proposed. The eel was divided into front and rear parts. For the first half, this paper used the projected area to build a weight model, and, for the second half, this paper used the body length to build a weight model. Then, the front and back models were combined to realize the weight measurement of the whole eel. The weighing model equation is as follows:

$$\begin{cases} G_{s\_front}(S) = a_1 S_{front} + b_1 \\ G_{l\_back}(L) = a_2 L_{back} + b_2 \\ G = G_{s\_front}(S) + G_{l\_back}(L) \end{cases} \tag{3}$$

where, G_{s_front} is the measured weight of the first half of the eel, g; a_1, b_1 are coefficients; G_{l_black} is the measured weight of the second half of the eel, g; a_2 and b_2 are coefficients; G is the overall measured weight of the eel, g.

2.3.2 Analysis of the relationship between division ratio and weight

For the division ratio of the front part and the back part of the eel, the appropriate division position was first selected. From the head of the eel to the division position is the first half. For this part, this paper used the projected area to build a mathematical model of the eel weight. From the division position to the tail of the eel is the second half, and for this part, this paper used the length of the skeleton to establish a mathematical model of the eel weight. By dividing the eel, the influence of the eel's tail posture on the weight calculation is avoided. Assuming that the length of the eel sample is L, cm, and the length of the eel from the head to the division point is l_{front}, cm, then the eel division ratio coefficient $p=l_{front}/L$.

The body shape of an eel is similar to a cylindrical shape, the content of the muscle and fat of each part of the fish is different, and the weight is related to the volume and density. To accurately obtain the eel weight distribution model, it was necessary to obtain the corresponding relationship between the density, volume, and mass of each part of the eel. Assuming that the length of the eel sample is L, the density is ρ, the weight is G, and the volume is V, then,

$$G = \rho V = \rho \int_0^L A(x)\,\mathrm{d}x,\ x \in (0, L) \tag{4}$$

where, $A(x)$ is the cross-sectional area, cm^2.

For the eel divided by the division ratio ρ, its weight G is,

$$G = \rho V_{front} + \rho V_{back} \tag{5}$$

where, V_{front} is the volume of the front part of the eel, cm^3; V_{back} is the volume of the back part of the eel, cm^3.

In the 2D image, the weight of the eel is directly related to the projected area and body length. At the same time, the shape of the eel is similar to a cylinder, and its weight model can be simplified to

calculate the mass of a cylinder. In this paper, the weight of the eel unit projected area was calculated from the first half of the projected area and the corresponding weight of the part, and defined as the area density ρ_s. The weight of the eel per unit body length was calculated from the body length of the latter half and the corresponding weight of this part, which was defined as the body length density ρ_l. For an eel with radius r, it has:

$$G_{\text{front}} = \rho V_{\text{front}} \approx \frac{\pi}{2} r\rho S_{\text{front}} \Rightarrow \rho_s S_{\text{front}} \tag{6}$$

$$G_{\text{back}} = \rho V_{\text{back}} \approx \pi r^2 \rho L_{\text{back}} \Rightarrow \rho_l L_{\text{back}} \tag{7}$$

2.3.3 Eel division experiments

Affected by the changes in the movement of living eels, the posture of the tail position causes the area of the projected image to change. Therefore, experiments were carried out on the two postures of the eel tail, both vertical and flat. First, the head of the eel projection image was used as the starting direction, and the division experiment was performed with a fixed step length. The width of 20 pixels was set as the step size and performed division in sequence to obtain a total of 62 groups of images. Figure 9 shows the 10th, 20th, 35th, and 50th divided images.

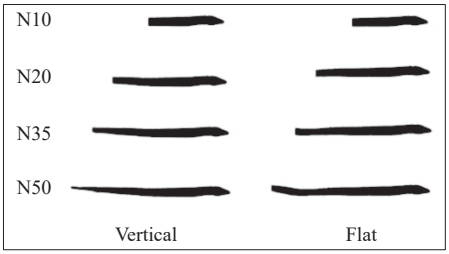

Figure 9 Division of eel projection images.

For the divided images in the two postures, the difference in the projected area was calculated. After calculation, before the 45th group, the difference in the projection area of the two poses was small and can be ignored. Figure 10 shows the changes in the projected area of groups 45 to 62.

From Figure 10, the area difference in the 45th to 50th groups was relatively small, and the area difference change rate was less than 2. After the 50th group, the area difference increased, and the change rate of the area difference increased significantly. Therefore, the sudden change in the projection area caused by the posture of the eel's tail occurred between the 45th and 50th groups of positions. Observation showed that, in the 48th group, the change rate of the area difference changed from 0.55 to 1.75, and the change was significant; thus, the 48th group was selected as the reference position of the division ratio coefficient. The calculation shows that the division ratio coefficient at this position was p=0.77.

To determine the area density ρ_s and body length density ρ_l of the eel object in this paper, different division scale factors were designed to carry out the division experiment of the eel entity. The division experiment of the eel projection image showed that when the division ratio was about 0.77, the eel's projected area had a significant shape mutation. Therefore, the division ratio was set to 0.70, 0.75, 0.80, and 0.85 for entity division experiments, and obtained the optimal division ratio coefficient through data analysis.

A randomly selected eel was used as the experimental subject. After measurement, the actual weight of the selected eel was 362 g, and the actual body length of the eel was 635 mm. The body of the selected eel was generally cylindrical and gradually transitioned to a flat body shape at the tail. The eel was divided according to the

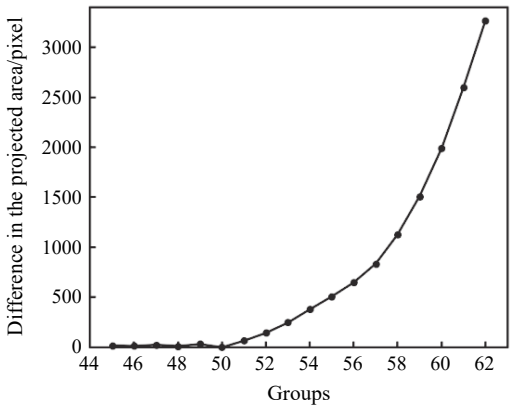

a. Difference in the projected area of the eel with two postures

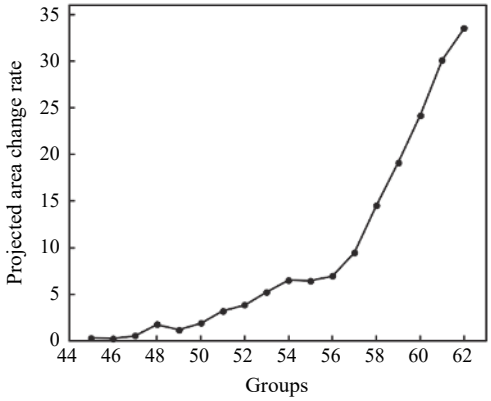

b. Change rate of the difference in the projected area

Figure 10 Change graph of the difference in projected area

proportions set by the body length. Figure 11 shows the division results of different division scale factors.

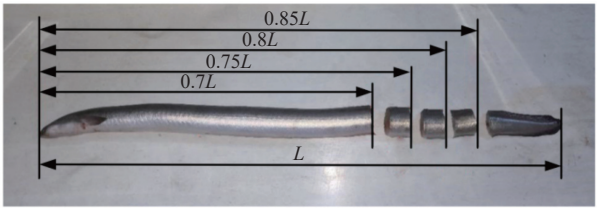

Figure 11 Division results of different division scale factors of eel segmentation

By weighing the divided eel, the weight of the front and back parts of the eel corresponding to each division ratio coefficient were obtained. At the same time, the eel image was divided according to the set division ratio coefficient, and the eel projection area and body length corresponding to each division ratio coefficient were calculated. From Equations (6) and (7), the weight of an eel is related to the projected area and length of an eel. At the same time, for the same species of eel, the area density and length density should vary within a certain range, and the weight can be measured by a general area density and general length density calculation. Thereby, an equation was developed to calculate the weight of an eel.

$$G_{\text{front}} = \rho_{s\_\text{test}} S_{\text{front}} = \frac{\rho'_{s\_\text{test}}}{k_{s\_\text{test}}} \cdot k_s S'_{\text{front}} \tag{8}$$

$$G_{\text{back}} = \rho_{l\_\text{test}} L_{\text{back}} = \frac{\rho'_{l\_\text{test}}}{\sqrt{k_{s\_\text{test}}}} * \sqrt{k_s} L'_{\text{back}} \tag{9}$$

where, G_{front} is the measured weight of the first half of the eel, g;

G_{back} is the measured weight of the second half of the eel, g; S'_{front} is the projected pixel area of the front half of the eel, pixel^2; L'_{back} is the projection skeleton length of the second half of the eel, pixel; ρ'_{s_test} is the pixel density per unit area, cm^2/pixel; ρ'_{l_test} is the pixel density per unit length, cm/pixel.

The specific data corresponding to the division ratio coefficients of each algorithm in the experiment are listed in Table 2.

Table 2 Data of eel division ratio coefficients of each algorithm

Scale factor	Weight (front/rear)/g	Front half area/pixels	Back half-length/pixels	Area density ρ'_s/g·pixel^{-1}	Length density ρ'_l/g·pixel^{-1}
0.70	310/52	61 697	363	199.02^{-1}	6.98^{-1}
0.75	328/34	64 427	303	196.42^{-1}	8.91^{-1}
0.80	341/21	67 049	242	196.62^{-1}	11.52^{-1}
0.85	351/11	69 612	181	198.32^{-1}	16.45^{-1}

In this study, the scaling method was adopted to calculate the area ratio between the real world and the image world, and the area ratio factor was calculated by a block of a certain size placed beside the experimental eel, namely: $k_s = S_{ref}/S'_{ref}$. For this experiment, the actual area of the placed block was S_{ref}=5776 mm^2, and the area on the map was S'_{ref} = 28 224 pixels, and thus k_{s_test}=4.8864^{-1} mm^2/pixel.

2.3.4 Model establishment

The eel area density and body length density calculated from the experiment were substituted into Equations (8) and (9) to obtain a general eel weight calculation model. Specifically, the weight of the front part of the eel was obtained from the area density and the area of the front part of the eel, and the weight of the back part was obtained from the length density and the length of the back part. The total weight of the complete eel was obtained by the sum of the weight of the two parts. The above weight measurement model equation is as follows:

$$\begin{cases} G_{s\_front}\left(S'_{front}\right) = \dfrac{\rho'_{s\_test}}{k_{s\_test}} \cdot k_s S'_{front} \\ G_{l\_back}\left(L'_{back}\right) = \dfrac{\rho'_{l\_test}}{\sqrt{k_{s\_test}}} \cdot \sqrt{k_s} L'_{back} \\ G = G_{s\_front}(S') + G_{l\_back}(L') \end{cases} \tag{10}$$

where, $G_{s\_front}\left(S'_{front}\right)$ is the eel weight measurement model based on area; $G_{l\_back}\left(L'_{back}\right)$ is the weight measurement model of the second half of the eel based on body length.

From Table 2, the area density and body length density corresponding to different division ratio coefficients were different. To determine the optimal division scale factor, the different forms of eel images were subjected to image division experiments according to the ratios of 0.70, 0.75, 0.80, and 0.85. Figure 12 shows the images of the experimental eels in different poses.

The sample images in different poses were segmented according to the division scale factors of 0.70, 0.75, 0.80, and 0.85. The area of the front part and the length of the back part were calculated after the division and substituted into the model Equation (13). Finally, the difference between the measured weight and the actual weight corresponding to each division ratio coefficient was calculated. On this basis, the variance between the measured weight and the actual weight under different posture images and different division scale factors was calculated. When the variance was the smallest, this indicated that the current division scale factor had the best adaptability.

The calculation showed that when the sum of variance was the smallest, the algorithm division scale factor value was 0.745, which was recorded as the general division scale factor. The area density corresponding to the general division scale factor was 196.54^{-1} g/pixels, and the body length density was 8.72^{-1} g/pixels. Substituting this into Equation (10), the general weight measurement model equation of experimental eels was obtained as,

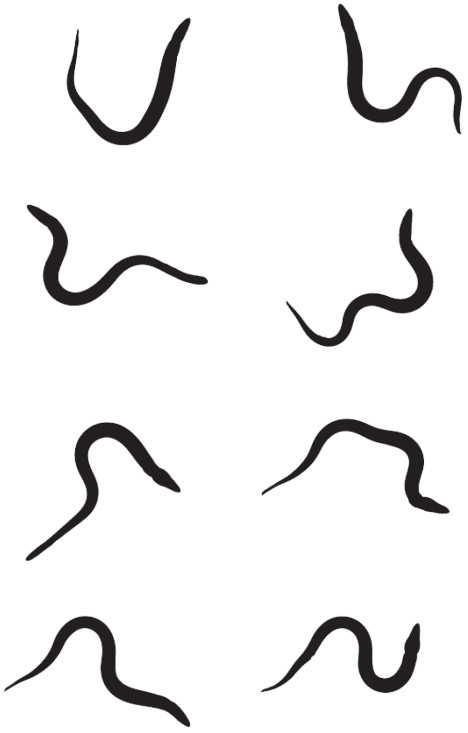

Figure 12 Different posture images of eels

$$G = 40.222^{-1} k_s S'_{front} + 3.945^{-1} \sqrt{k_s} L'_{back} \tag{11}$$

2.4 Model analysis and calibration

For Equation (14), the general weight measurement model was based on eels weighing 362 g. Due to the differences in the body types of eels with different weights, the body types of eels with the same weight may also be different. Therefore, an experiment was conducted to apply the current eel weight measurement model to other eels of different weights for testing. The test results are shown in Table 3. For the results, the general weight measurement model based on eels weighing 362 g was used for weight detection of eels with various weights, and the detection error varied with the weight of the test sample. To eliminate errors caused by the adaptability of the model, this study corrected the general weight measurement model.

Table 3 Weight ratio results

No.	Actual weight/g	Test weight/g	Errors/g	Coefficient of deviation
1	184.00	228.51	−44.51	1.242
2	229.00	257.71	−28.71	1.125
3	286.00	299.10	−13.10	1.046
4	337.00	329.28	7.72	0.977
5	375.00	359.01	15.99	0.957
6	439.00	377.40	61.60	0.860
7	461.00	395.46	65.54	0.858
8	540.00	430.91	109.09	0.798
9	654.00	487.86	166.14	0.746

From Table 3, when the weight of the test sample was 184.00 g, the ratio of the average measured weight to the actual weight was 1.242. When the weight of the test sample was 654 g, the ratio of

the average measured weight to the actual weight was 0.746. As the detection weight increased, the coefficient of deviation continued to decrease. Therefore, a functional equation between the measured weight and the coefficient of deviation was established. The variation of the deviation coefficient with weight is shown in Figure 13.

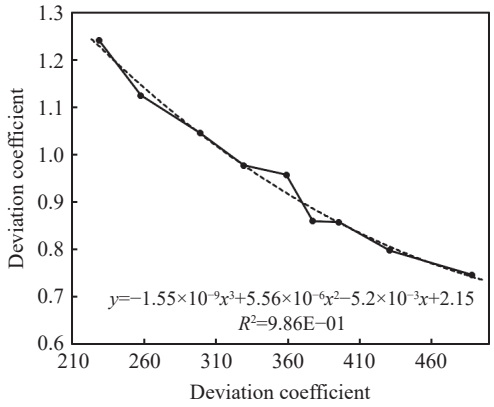

Figure 13 Relationship between the deviation coefficient and the measured weight

A 3-order fitting was performed on the deviation coefficient and the measured weight. The function equation is,

$$Y(G) = -1.55\times10^{-9}G^3 + 5.56\times10^{-6}G^2 - 0.0052G + 2.15 \quad (12)$$

where, G is the measured weight; $Y(G)$ is the coefficient of deviation.

Equation (11) general weight measurement model was corrected, and the corrected weight detection model equation set is,

$$\begin{cases} G = 40.222^{-1}k_s S'_{\text{front}} + 3.945^{-1}\sqrt{k_s}L'_{\text{back}} \\ G_{\text{cor}} = G/Y(G) \end{cases} \quad (13)$$

where, G is the overall measured weight of the eel before calibration; G_{cor} is the overall measured weight of the eel after calibration; $Y(G)$ is the deviation correction fitting equation.

3 Results

To verify the effectiveness of the method proposed in this paper, nine live eels with different weights and shapes were randomly selected to collect images at different times for experiments, and the measured weight of the eels was obtained through the series of processing procedures proposed in this study. The computer hardware and software parameters used in the experiment included an Intel i7-4210U @ 1.70 GHz CPU, 4 GB memory, and a Windows 7 operating system, and MATLAB programming language was used for programming.

The measured weight calculated by the system was compared with the actual measurement results to prove the accuracy of the system. The root mean square error (RMSE) and mean absolute percentage error (MAPE) of the system detection results were calculated as follows:

$$\text{RMSE} = \sqrt{\frac{1}{n}\sum_{i=1}^{n}(x_{si} - x_{mi})^2} \quad (14)$$

$$\text{MAPE} = \frac{1}{n}\sum_{i=1}^{n}\frac{|x_{si} - x_{mi}|}{x_{mi}} \times 100\% \quad (15)$$

where, x_{si} is the system measurement result, g; x_{mi} is the manual measurement result, g.

3.1 Image processing results

To measure the weight of the eel based on the image, the collected images were first preprocessed to obtain the area and skeleton length. On this basis, the eel weight was estimated through the designed weight model. Figure 14 shows the five sets of results of the image processing steps, including, from left to right, the original images of eels, the segmentation results, and the skeleton length results of the segmented images. The results showed the excellent performance of the image processing method proposed in this study.

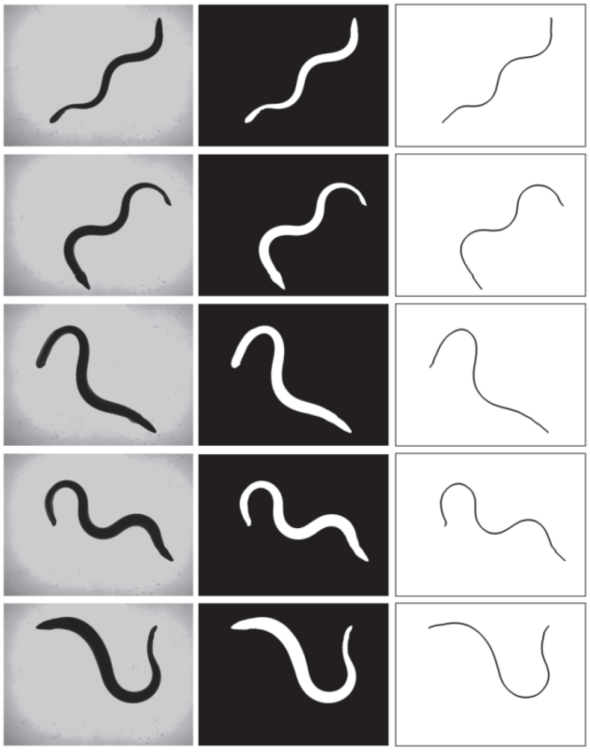

a. Original diagram b. Binary diagram c. Skeleton diagram

Figure 14 Results of image processing

3.2 Weight measurement results

For the obtained images, the weight of the eels was calculated according to the designed pipeline. To verify the accuracy of the designed algorithm, the values obtained by the system were compared to the results of the manual measurements. Finally, a regression analysis was performed on the data, and the root mean square error and the mean absolute percentage error were calculated.

For the weight (Figure 15), the RMSE was 12.94 g, and the

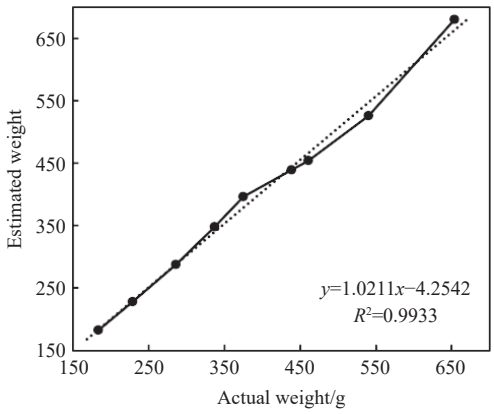

Figure 15 Regression analyses comparing the actual weight versus the estimated weight

MAPE was 2.12%, and the fitting equation showed that the system had a strong explicit correlation between the estimated weight and the actual weight, which demonstrated the accuracy of the system's calculation.

To verify the robustness of the system, images of each eel in different poses were collected separately, and each eel was collected 15 times. The weight of each eel was calculated separately and calculated the average absolute error and average relative error of each eel was. The specific results are listed in Table 4.

Table 4 Results of the system measurements

No.	Mean absolute error/g	Mean relative error/%
1	7.69	4.2
2	5.76	2.6
3	7.71	2.6
4	12.65	3.5
5	20.91	5.2
6	13.49	3.1
7	7.92	1.8
8	16.67	3.2
9	29.40	4.3
Average	14.26	3.4

For the measured weight of the system, the average absolute error between the actual weight and the measured weight was 14.26 g, the maximum relative error of a single weight was 5.2%, the minimum was 1.8%, and the average relative error was 3.4%. In summary, the experimental results demonstrated the accuracy and robustness of this method.

4 Discussion

In this study, a novel method for image-based weight measurement of live eels was proposed. The method includes the steps of image acquisition, image pre-processing, weight model establishment, model error analysis, and correction. The experimental results showed that the method had a small error and met the technical requirements of actual eel production. Compared with other methods, the method is less costly and more reliable in terms of portability. At the same time, this method still has some limitations.

1) During the test, the gills of live eels had low-frequency opening and closing movements, as shown in Figure 16, which shows two different states of gills opening (Figure 16a) and closing (Figure 16b) of the same eel, and the opening and closing of gills could lead to inaccurate calculation of the projection area of the eel. In future work, in order to reduce the calculation inaccuracy caused by the gill motion of eels, consider segmenting the eel by head, body, and tail to avoid the detection error caused by gills.

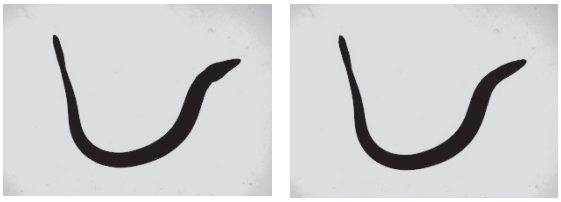

a. Opening b. Closing

Figure 16 Gill opening and closing action diagram of live eel

2) This real experiment used a fixed division ratio coefficient, which was determined as 0.745 based on the eel with a weight of 362 g. Then the division ratio coefficient corresponding to 362 g eel was applied to other weights of eels. Although this method protected the operational efficiency of the system, the fixed division coefficient would cause certain errors for eels with large size differences, and for other weights of eels There may be more suitable division ratio coefficients, therefore, in future work, the dynamic division coefficients will be studied to further improve the accuracy of the weight measurement model.

3) In the image acquisition process, a backlight real-time eel image acquisition device was designed in this study to acquire 2D projection images of eels using backlight transmission technology, which solves the problems of instability and reflection interference of external light sources. However, when the backlight was not strong enough, the double fin projection of the eel generated disturbance in the image segmentation, as shown in Figure 17. Therefore, further, more effective image segmentation methods are needed to improve the segmentation accuracy. Future work can use eel skeleton and contour maps to analyze the shape and movement of eels to improve the refinement of eel classification, as well as to study the identification and separation of fins to reduce the effect of disturbance caused by fins.

Figure 17 Binary image with double fin disturbance.

4) Extraction of the image skeleton remains a challenge. Due to the smooth appearance of eels, the skeleton can be extracted efficiently based on a sequential iterative algorithm. However, this algorithm may lead to the loss of skeleton endpoints, which results in the computed skeleton length being smaller than the actual skeleton length. In recent years, researchers have investigated different skeleton extraction schemes. However, exploring effective skeleton extraction techniques is still a topic that needs further research.

5 Conclusions

To meet the requirements of the industry, this study proposed a novel method for image-based weight measurement of live eels. The method effectively reduces the damage rate of live eels by non-contact detection of live eel weight. At the same time, no complicated mechanical and electronic weight measurement devices are required, and weight errors caused by eel movement are avoided. First, a backlit table was designed to capture eel images, and then the projected area and skeleton length of eel images were obtained by image pre-processing. Based on this, an eel weight measurement model combining the projected area and skeleton length was proposed based on the body characteristics of the eel. The general weight measurement model of eels was established by eel segmentation experiments. Finally, eels of different weight ranges were selected for model error verification, and the modified mathematical model of eel weight was obtained. When comparing the calculated results of this system with the actual measurement results, the root mean square error was 12.94 g and the average absolute percentage error was 2.12%. The results show that this

study provided a convenient, fast, and low-cost method for non-contact weight measurement of live eels and provided a research basis for non-contact weight measurement of live eels. At the same time, the weight prediction model established by combining the pixel area and skeleton length of eels through segmentation of live eels in this study also provided a new processing idea for weight measurement of irregular objects similar to eels.

Acknowledgements

This work was supported by the Research and Promotion of Key Technologies of Intelligent Equipment for Special Agricultural Products (Eels, *Citrus reticulata* 'Chachi') of Guangdong Province (No. 163-2019-XMZC-0009-02-0057), the National Natural Science Foundation of Guangdong Province, China (Grant No. 2018B030306026), the Regular Institutions of Higher Education Key Field Project of Guangdong Province, China (Grant No. 2019KZDZX1001), Guangdong Basic and Applied Basic Research Foundation (Grant No. 2020A1515110191).

[References]

[1] Cheng J-H, Dai Q, Sun D-W, Zheng X-A, Liu D, Pu H-B. Applications of non-destructive spectroscopic techniques for fish quality and safety evaluation and inspection. Trends in Food Science & Technology, 2013; 34(1): 18–31.

[2] Koltes J E, Cole J B, Clemmens R, Dilger R N, Kramer L M, Lunney J K, et al. 2019. A vision for development and utilization of high-throughput phenotyping and big data analytics in livestock. Frontiers in Genetics, 2019; 10: 1197.

[3] Liakos K G, Busato P, Moshou D, Pearson S, Bochtis D. Machine learning in agriculture: A review. Sensors, 2018; 18(8): 2674.

[4] Ma X D, Zhu K X, Guan H O, Feng J R, Yu S, Liu G. High-throughput phenotyping analysis of potted soybean plants using colorized depth images based on a proximal platform. Remote Sensing, 2019; 11(9): 1085.

[5] Banerjee B P, Spangenberg G, Kant S. Fusion of spectral and structural information from aerial images for improved biomass estimation. Remote Sensing, 2020; 12(19): 3164.

[6] Niu Y X, Zhang L Y, Zhang H H, Han W T, Peng X S. Estimating above-ground biomass of maize using features derived from UAV-based RGB imagery. Remote Sensing, 2019; 11(11): 1261.

[7] Calixto R, Neto L G P, de Silveira Cavalcante T, Aragão M F, Silva E D. A computer vision model development for size and weight estimation of yellow melon in the Brazilian northeast. Scientia Horticulturae, 2019; 256: 108521.

[8] Cheng H, Damerow L, Sun Y R, Blanke M. Early yield prediction using image analysis of apple fruit and tree canopy features with neural networks. Journal of Imaging, 2017; 3(1): 6.

[9] Rahman M M, Robson A, Bristow M. Exploring the potential of high resolution WorldView-3 imagery for estimating yield of mango. Remote Sensing, 2018; 10(12): 1866.

[10] Jung D-H, Park S H, Han X Z, Kim H-J. Image processing methods for measurement of lettuce fresh weight. Journal of Biosystems Engineering, 2015; 40(1): 89–93.

[11] Koirala A, Walsh K B, Wang Z L, McCarthy C. Deep learning - Method overview and review of use for fruit detection and yield estimation. Computers and Electronics in Agriculture, 2019; 162: 219–234.

[12] Zhang Z Q. Research on freshwater fish species identification and weight prediction based on machine vision. Master dissertation. Wuhan:Huazhong Agricultural University, 2011; 66p. (in Chinese)

[13] Li L, Guo X Y. Research on fish classification method based on computer vision. Journal of Inner Mongolia Agricultural University (Natural Science Edition), 2015; 36(5): 120–124. (in Chinese)

[14] Viazzi S, Van Hoestenberghe S, Goddeeris B M, Berckmans D. Automatic mass estimation of Jade perch *Scortum barcoo* by computer vision. Aquacultural Engineering, 2014; 64: 42–48.

[15] Ma G Q, Tian Y C, Li X L. Individual weight estimation of narrow-bodied tongue sole based on irregular image area measurement. Microcomputers and Applications, 2016; 35(16): 67–71. (in Chinese)

[16] Wang L, Sun C H, Li W Y, Ji Z T, Zhang X, Wang Y Z, et al. Establishment of broiler quality estimation model based on depth image and BP neural network. Thransactions of the CSAE, 2017; 33(13): 199–205. (in Chinese)

[17] De Wet L, Vranken E, Chedad A, Aerts J M, Ceunen J, Berckmans D. Computer-assisted image analysis to quantify daily growth rates of broiler chickens. British Poultry Science, 2003; 44(4): 524–532.

[18] Schofield C P, Marchant J A, White R P, Brandl N, Wilson M. Monitoring pig growth using a prototype imaging system. Journal of Agricultural Engineering Research, 1999; 72(3): 205–210.

[19] Yang Y, Teng G H, Li B M, Shi Z X. Measurement of pig weight based on computer vision. Transactions of the CSAE, 2006; 22(2): 127–131. (in Chinese)

[20] Fu W S, Teng G H, Yang Y. Research on three-dimensional model of pig's weight estimating. Transactions of the CSAE, 2006; 22(S2): 84–87. (in Chinese)

[21] Alikhanov J, Penchev S M, Georgieva T D, Modazhanov A, Shynybay Z, Daskalov P I. An indirect approach for egg weight sorting using image processing. Journal Of Food Measurement And Characterization, 2018; 12: 87–93.

[22] Wang J F, Luo X W, Hong T S, Ge Z Y. Application of computer vision technology in detecting mango weight and surface bruise. Transactions of the CSAE, 1998; (4): 186–189. (in Chinese)

[23] Kalantar A, Edan Y, Gur A., Klapp, l. A deep learning system for single and overall weight estimation of melons using unmanned aerial vehicle images. Comput Electron Agr, 2020; 178.

[24] Dowlati M, Mohtasbi S S, de la Guardia M. Application of machine-vision techniques to fish-quality assessment. TrAC Trends in Analytical Chemistry, 2012; 40: 168–179.

[25] Dutta M K, Issac A, Minhas N. Image processing based method to assess fish quality and freshness. Journal of Food Engineering, 2016; 177: 50–58.

[26] Otsu N. A threshold selection method from gray-level histograms. IEEE Transactions on Systems Man & Cybernetics, 2007; 9(1): 62–66.

[27] Liu G L, Reda F A, Shih K J, Wang T-C, Tao A, Catamzaro B. Image inpainting for irregular holes using partial convolutions. In: Computer Vision – ECCV 2018, Springer, 2018; 89–105.